

Reconstruction methods of Axial and Radial Leakage for 2D/1D fusion method

Liang Liang^a, Liu Zhouyu^{a,*} and Wu Hongchun^a

^a*Xi'an Jiaotong University, No.28, Xianning West Road, Xi'an, Shaanxi, 710049, P.R. China*
zhouyuliu@mail.xjtu.edu.cn

1. Introduction

The 3D whole-core heterogenous transport calculation plays a very important role in high fidelity calculations for reactor physics, among which, 2D/1D fusion method^[1] (including 2D/1D method^[2]) is one of the most promising methods. In conventional 2D/1D fusion method, the axial leakage is flat on the top/bottom surfaces of the homogenous cells and the radial leakage is flat along the axial direction of the 2D calculation plane, so these approximations will get some accuracy lost. This work is to analysis and minus the errors these approximations bring. In 1D calculation the radial leakage is fitted along axial direction while in 2D calculation the distribution of axial leakage is also introduced. The numerical results indicate that these two improvements reduce the errors brought by the flat leakage approximation.

2. 2D/1D Fusion Method

The multi-group neutron transport equation can be written as

$$\xi_m \frac{\partial \psi_g(\mathbf{r}, \Omega_m)}{\partial x} + \eta_m \frac{\partial \psi_g(\mathbf{r}, \Omega_m)}{\partial y} + \mu_m \frac{\partial \psi_g(\mathbf{r}, \Omega_m)}{\partial z} + \Sigma_{t,g}(\mathbf{r}) \psi_g(\mathbf{r}, \Omega_m) = Q_g(\mathbf{r}, \Omega_m) \quad (1)$$

The 2D equation of 2D/1D fusion method is obtained by integrating Eq. (1) over $[z_{k-1}, z_{k+1}]$.

$$\xi_m \frac{\partial \psi_{g,m,k}(x, y)}{\partial x} + \eta_m \frac{\partial \psi_{g,m,k}(x, y)}{\partial y} + \Sigma_{t,g,k}(x, y) \psi_{g,m,k}(x, y) = Q_{g,k}(x, y) - TL_{g,m,k}^{Axial}(x, y) \quad (2)$$

where, the axial leakage is

$$TL_{g,m,k}^{Axial}(x, y) = \frac{\mu_m}{\Delta z_k} [\psi_{g,m,k+1/2}(x, y) - \psi_{g,m,k-1/2}(x, y)]$$

The 1D equation is got by integrating Eq. (1) over $[x_{i-1}, x_i], [y_{j-1}, y_j]$

$$\mu_m \frac{d\psi_{g,m}^p(z)}{dz} + \Sigma_{t,g,p}(z) \psi_{g,m}^p(z) = Q_g^p(z) - TL_{g,m,p}^{Radial}(z) \quad (3)$$

where, the radial leakage is,

$$TL_{g,m,p}^{Radial}(z) = \frac{\xi_m}{\Delta x} [\psi_{g,m,x+}^p(z) - \psi_{g,m,x-}^p(z)] + \frac{\eta_m}{\Delta y} [\psi_{g,m,y+}^p(z) - \psi_{g,m,y-}^p(z)]$$

For the conventional 2D/1D method, the 3D geometry is divided into several layers for 2D calculations, and then divided into parallel pins for 1D calculation, as show in Fig.1. 2D calculations supply the radial leakage for 1D calculations, while 1D calculations supply axial leakage. Fig. 2 shows the calculation flow of 2D/1D transport code MOCHA2D1D.

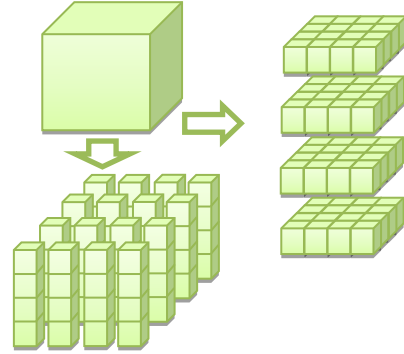


Fig.1. 2D/1D meshing figure

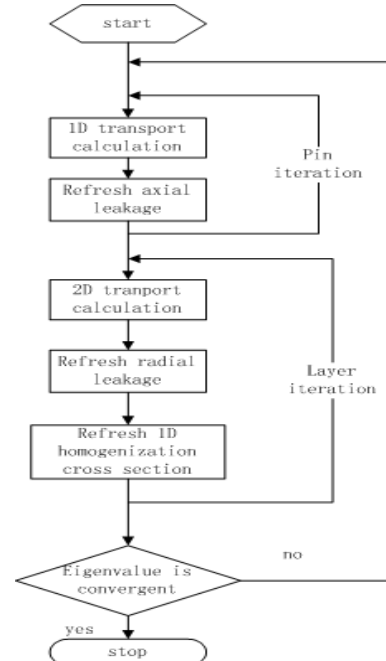


Fig. 2 MOCHA-2D1D calculation flow

3. Radial Leakage Reconstruction

For the 2D calculations, the resulting leakage between cells is flat along axial direction. However, the mesh is much finer than the height of 2D layers. This leakage distribution along axial direction might change significantly in some case. So applying Radial leakage reconstruction along axial direction is needed. Here, Sn difference method is applied for the 1D

calculation, and the radial leakage is fitted using a quadratic polynomial.^[3,4] Choosing Sn method is to guarantee no approximation on angle. Since 1D calculation does not take much time, the differential method is easy to get fine mesh flux.

$$L^n(\xi) = \sum_{i=0}^2 l_i^n P_i(\xi) \quad (4)$$

Where,

$$P_0 = 1, P_1 = \xi, P_2 = 3\xi^2 - 1/4$$

The coefficients (l_i^n) are determined from radial leakage integral on layer $n-1, n$, and $n+1$. The coefficients are obtained by

$$l_0^k = TL_{g,k}^{Radial}$$

$$l_1^k = \frac{\Delta z_k}{d} \left[\begin{array}{l} z_{k-1} (TL_{g,k+1}^{Radial} - TL_{g,k}^{Radial}) \\ + z_{k+1} (TL_{g,k}^{Radial} - TL_{g,k-1}^{Radial}) \end{array} \right] \quad (5)$$

$$l_2^k = \frac{(\Delta z_k)^2}{d} \left[\begin{array}{l} (\Delta z_{k-1} + \Delta z_k) (TL_{g,k+1}^{Radial} - TL_{g,k}^{Radial}) \\ - (\Delta z_{k+1} + \Delta z_k) (TL_{g,k}^{Radial} - TL_{g,k-1}^{Radial}) \end{array} \right]$$

where,

$$z_i = (\Delta z_k + \Delta z_i)(\Delta z_k + 2\Delta z_i)$$

$$d = (\Delta z_{k-1} + \Delta z_k)(\Delta z_k + \Delta z_{k+1})(\Delta z_{k-1} + \Delta z_k + \Delta z_{k+1})$$

Using these coefficients, the radial leakage of each 1D fine mesh could be obtained. Fig. 3 shows the radial leakage distribution before and after fitting.

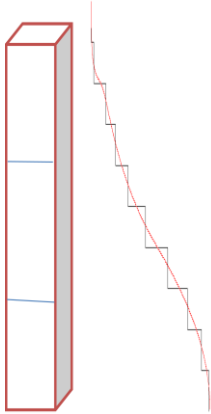


Fig.3.Radial leakage fitting along axial direction

4. Axial Leakage Reconstruction

According to the previous work of Prof. Cho^[1], choosing 2D flat source mesh as 1D calculation domain could obtain better results while the computation time and the memory consumption will increase, the memory consumption increase is the major restriction. So most 2D/1D codes choose a cell as the 1D calculation domain. To capturing the leakage distribution on the top/bottom surface of the cell, a method to reconstruct the 2D distribution of the axial leakage is introduced as Eq. (6). According to this expression, an assumption is introduced that the distribution of leakage on the top/bottom surface is the same for different angles. Then

the shape factor of each flat source mesh is obtained directly using the scalar flux of different layers. Multiplying this shape factor and the leakage could generate the axial 2D distribution.

$$TL_{g,m,k}^{Axial}(x, y) = \frac{\mu_m}{\Delta z_k} [\psi_{g,m,k+1/2}(x, y) - \psi_{g,m,k-1/2}(x, y)]$$

$$TL_{shad} = \frac{\mu_m}{\Delta z_k} [\phi_{k+1/2}(x, y) - \phi_{k-1/2}(x, y)] \quad (6)$$

$$\phi(x, y, \xi) = \sum_{i=0}^2 l_i^n P_i(\xi)$$

where,

$$P_0 = 1, P_1 = \xi, P_2 = 3\xi^2 - 1/4$$

$$\phi_0^k = \phi_k$$

$$\phi_1^k = \frac{\Delta z_k}{d} \left[\begin{array}{l} z_{k-1} (\phi_{k+1} - \phi_k) \\ + z_{k+1} (\phi_k - \phi_{k-1}) \end{array} \right] \quad (7)$$

$$\phi_2^k = \frac{(\Delta z_k)^2}{d} \left[\begin{array}{l} (\Delta z_{k-1} + \Delta z_k) (\phi_{k+1} - \phi_k) \\ - (\Delta z_{k+1} + \Delta z_k) (\phi_k - \phi_{k-1}) \end{array} \right]$$

where,

$$z_i = (\Delta z_k + \Delta z_i)(\Delta z_k + 2\Delta z_i)$$

$$d = (\Delta z_{k-1} + \Delta z_k)(\Delta z_k + \Delta z_{k+1})(\Delta z_{k-1} + \Delta z_k + \Delta z_{k+1})$$

$$\phi_{k+1/2}(x, y) = \phi(x, y, 1/2)$$

$$\phi_{k-1/2}(x, y) = \phi(x, y, -1/2)$$

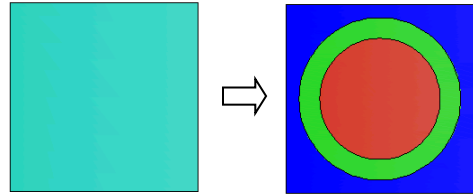


Fig.4 Axial leakage 2D distribution calculation

Using the shape factor of axial leakage for each cell, the 2D distribution of axial leakage on each pin could be obtained as shown in Fig. 4. Since the problem we calculate is small, the memory increasing is not the key restriction. But we can estimate the additional memory. The axial leakage array of the current calculating layer becomes larger, the multiple is the number of flat source mesh. The axial leakage is not isotropic, only the shape factor of axial leakage on each direction is same.

5. Numerical Result

In order to test the reconstruction methods, a 3x3 pin problem is designed, and the pin geometry is shown in Fig. 5. The pitch of each pin is 1.0cm, and the height is 25cm. Cross sections are listed in Table I. Rectangle pin geometry is used to eliminating the errors introduced by the homogenization approximation of the 1D calculation. 4 cases are calculated to compare the reconstruction effect: 1) with radial leakage reconstruction, 2) with

axial leakage reconstruction, 3) with both axial and radial reconstruction, 4) reference case. For all cases, 5 by 5 meshing is adopted for each pin during the calculation.

In the reference case, 1D calculations are performed for each flat-source-region. For other case 1D calculations are performed for one pin. 40 rays for one pin on each direction, 6 azimuthal angles and 4 polar angles in an octant, 10 layers are used. The results are shown below.

In the first case, 1D calculations with radial leakage reconstruction are performed for each flat-source-region. 40 rays for one pin on each direction, 6 azimuthal angles and 4 polar angles in an octant, 5 layers are used. The results of with and without radial leakage reconstruction are shown in Table II and Table III.

In the second case, 1D calculations with radial leakage reconstruction are performed for each pin. 200 rays for one pin on each direction, 6 azimuthal angles and 4 polar angles in an octant, 10 layers are used. The results of with and without axial leakage reconstruction are shown in Table IV and Table V.

In the third case, 1D calculations with radial leakage reconstruction are performed for each pin. 200 rays for one pin on each direction, 6 azimuthal angles and 4 polar angles in an octant, 5 layers are used. The results of with or without both radial and axial leakage reconstruction are shown in Table VI and Table VII.

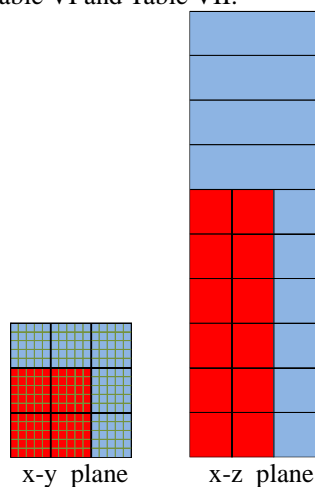


Fig.5 reference case configuration

Table I cross section

Cross section	Total	Nu fission	fission	Scatter
Fuel	2.81E+00	8.54E-01	3.5E-01	2.26E+00
Rod	6.44E+00	0.00E+00	0.0E+00	3.14E+00
Coolant	6.37E+00	0.00E+00	0.0E+00	6.31E+00

In first case, the error of eigenvalue decreases by 20 pcm with the radial leakage reconstruction, and the pin power of fifth layer, where the layer of maximum pin power is, has not big difference because both of them are accuracy enough. The results indicate that the radial leakage is not the major source of error in this case.

From the results of the second case, it could be found that flat axial leakage introduced about 100 pcm error in eigenvalue and 0.5% error in maximum pin powers layer. Axial leakage reconstruction gives a more accurate

distribution of leakage of the top/bottom surface, which brings 40 pcm improvement in eigenvalue and reduces the pin power error significantly. So in this case the domain error source is the flat axial leakage.

In the third case, both axial leakage reconstruction and radial leakage reconstruction are applied. The error of eigenvalue is decrease about 15 pcm, because these two methods correct the eigenvalue in opposite directions. The pin power of fifth layer still improved a lot. The results indicate that when the leakage is large and changes greatly, reconstruction methods could improve the result.

Table II eigenvalue of first case

First case	eigenvalue	error/pcm
reference	1.25899	-
no reconstruction	1.25840	-59
radial leakage Reconstruction	1.25860	-39

Table III pin power difference of 5th layer

First case	Error of pin power	
No reconstruction (%)	0.00	0.02
	-0.01	0.00
radial leakage reconstruction(%)	0.02	0.11
	-0.08	0.02

Table IV eigenvalue of second case

Second case	eigenvalue	Error/pcm
reference	1.25899	-
no reconstruction	1.26010	111
axial leakage Reconstruction	1.25972	73

Table V pin power difference of 10th layer

Second case	Error of pin power	
No reconstruction (%)	0.58	0.56
	0.58	0.58
axial leakage reconstruction(%)	0.09	0.07
	0.09	0.09

Table VI eigenvalue of third case

Third case	eigenvalue	Error/pcm
reference	1.25899	-
no reconstruction	1.26061	162
Both reconstruction	1.26046	147

Table VII pin power difference of 5th layer

Third case	Error of pin power	
No reconstruction (%)	-0.49	-0.39
	-0.58	-0.49
Both reconstruction(%)	0.00	0.04
	-0.02	0.00

6. Conclusions

Two improvements are proposed for the conventional 2D/1D fusion transport method, in which the radial leakage from the 2D calculation is fitted along axial direction for 1D Sn equation, and 2D distribution of the axial leakage from 1D calculation is fitted for the 2D MOC calculation. Both reconstructions contribute some improvements to the accuracy of the eigenvalue and pin powers. The effect of reconstruction is depended on the shape of true leakage. For the given problem, the radial leakage is the main source of the bias, so the reconstruction shows more improvements to the final results. More investigation will be performed for the pin powers closed to the moderator for the bigger problems. Next we will apply this method to C5G7 benchmark to test the performance.

References

1. Gil Soo Lee, Nam Zin Cho, "2D/1D fusion method solutions of the three-dimensional transport OECD benchmark problem C5G7 MOX", Progress in Nuclear Energy 48 (2006) 410-423.
2. Han Gyu Joo, Jin Young Cho, "Methods and Performance of a Three-Dimensional Whole-Core Transport Code DeCART", Chicago, Illinois, April 25-29, 2004, American Nuclear Society (CD-ROM).
3. Shane G. Stimpson, Benjamin S. Collins, "AXIAL TRANSPORT SOLVERS FOR THE 2D/1D SCHEME IN MPACT", Proc. PHYSOR 2014, The Westin Miyako, Kyoto, Japan, September 28 - October 3, 2014 (CD-ROM).
4. Mathieu Hursin, Brendan Kochunas, Thomas J. Downar, DeCART v2.05 Theory Manual. (November 2008)